An Analysis of Differentiation and Integration of Retinoid Transplantations in RCS Rats

Tej Kalakuntla, *Biological Sciences*
Johanes A. Santoso, *Public Health Sciences*

Authors

From the time they joined Professor Seiler's research group, Tej Kalakuntla and Johanes Santoso have been encouraged to pursue independent work. They proposed the research presented here and gained the experience of being involved in a project from its very beginning. Both Tej and Johanes are planning to continue on to medical school after graduation and feel that their work in Professor Seiler's lab has helped them move toward that goal.

Key Terms

- Immunofluorescence
- Macular Degeneration
- Photoreceptors
- Retinal Organoids
- Retinal Pigment Epithelium
- Stem Cells

Abstract

Nearly half of the vision related diseases in Western society are due to retinal degeneration. Most studies aim to prevent vision loss by treating early stages of retinal degeneration, but once the diseases progress and photoreceptors and retinal pigment epithelium (RPE) have late-stage degenerated, they need to be replaced with new cells. This study focuses on the hypothesis that sub-retinal transplantation of embryonically derived retinal progenitor sheets will lead to a restoration of photoreceptors and visual acuity in Royal College of Surgeons (RCS) rats that have a genetic defect in the RPE that leads to almost complete degeneration of their photoreceptors. Sub-retinal transplants were placed in the blind rats at the age of 7–8 weeks and were allowed to develop anywhere from 50 to 300 days before the rats were perfused. Testing was done by sectioning the eyes of RCS rats with transplant surgery. The sections were then stained and analyzed to demonstrate the presence of photoreceptors after transplantation. We found that, post-transplantation, RCS rats that would normally be without photoreceptors had significant numbers of rod and cone cells. These cells were then found to be associated mostly with the transplanted region, which was especially true in rats with late stage degeneration. Overall, it was clear that the hypothesis was supported.

Faculty Mentor

Tej Kalakuntla and Johanes Santoso analyzed retinal transplants to Royal College of Surgeons rats, a model of retinal degeneration, using a variety of antibodies and staining methods. Most retinal sheet transplants were derived human embryonic stem cells that had been developed into retinal organoids. Transplants were analyzed 2–7 months after transplantation. The data show that transplants develop new photoreceptors and integrate with the host retina. The students learned to work together as a team, as most experiments take longer time than 4 hours per day. They also learned how to troubleshoot experiments. Both students are heading for Medical School. Tej has already been accepted and Johanes will try to get to Medical School in the fall of 2020.

Magdalene Seiler
School of Medicine

Introduction

Age-related macular degeneration and retinitis pigmentosa are just two examples of retinal degenerative diseases, which account for 45% of vision related diseases in the Western world (Lim et al., 2012). The nature of the disease makes it very difficult to cure in later stages, since the retinal pigment epithelium (RPE) is so severely damaged that modern techniques, like gene therapy, are rendered ineffective (Liu et al., 2011). Because the function of RPE is to sustain retinal cells, a degeneration or dysfunction of RPE leads to a reduction of viable photoreceptors.

Since retinal degeneration leads to a loss of RPE cells and photoreceptors, one method that has been found effective in treating late stage retinal degeneration is to insert a sheet of retinal progenitor cells (RPCs) (Seiler and Aramant 2012). The effectiveness of this technique has been shown in multiple studies. Transplanting fetal retinal progenitor sheets into humans has led to an increase in visual acuity, meaning that the fetal retinal progenitor sheets do properly differentiate into photoreceptors that integrate with the remaining layers of the host retina. (Radtke et al., 2008) In addition, the transplantation of RPC sheets has been found to be an effective way to restore visual function in RD nude rats expressing a mutant rhodopsin (*rho S334ter-3*) (Seiler et al., 2014; Seiler et al., 2017).

Due to the relatively fast retinal degeneration rate of RD rats, however, they are not a perfect representation of human macular degeneration. Royal College of Surgeons (RCS) rats degenerate at a much slower rate and have a defect in their RPE that induce a loss of photoreceptors over time, making them more similar to human retinal degeneration (D'Cruz et al., 2000; Cuenca et al., 2005). Previous studies have found that the RCS rat demonstrates continual retinal degeneration over the course of 3–5 months (Adachi et al., 2016). We used an immunocompromised RCS rat model that was developed by crossing RCS rats with NIH nude rats (Thomas et al., 2016, ARVO abstract), so subject rats would be nude, be immunocompromised (transplant will not be rejected), and have retinal degeneration.

In this study, embryonic stem cells were differentiated into retinal organoids. Sheets dissected from organoids (RPC sheets) were transplanted into the RCS rat model by Dr. Magdalene Seiler. The differentiation of the RPC sheets was analyzed to establish that they had formed RPE, photoreceptors, and other retinal cells. The differentiation of RPC sheets was visualized via various staining techniques, including hematoxylin and eosin (H and E) staining and immunohistochemistry, using 3,3'-Diaminobenzidine (DAB) staining and immunofluorescence (IFA). The use of these techniques allowed us to identify various cell types, including rods (Rhodopsin), cone bipolar cells (Recoverin), red and green cone cells (Red Green Opsin), and human cells (Ku-80 and SC-121) (Seiler et al., 2017; McLelland et al., in revision). The hypothesis is that subretinal transplantation of embryonic RPC sheets will lead to a significant increase in photoreceptors, thus improving the visual acuity of RCS rats that have undergone retinal degeneration.

Materials and Methods

Animals

All experiments were carried out in accordance with the Institutional Animal Care and Use Committee at the University of California, Irvine, and were consistent with Federal guidelines. All of the animals used for testing were housed in a vivarium with individually filtered air for each cage. There were two to three rats per cage, depending on sex (two males per cage and three females per cage), and the rats were put on a 12-hour light/dark cycle, with an ambient temperature of 21.5 ± 0.8 °C and a relative humidity of 50%. RCS rats were genetically bred to be immunocompromised and have a mutation that leads to the degeneration of RPE, thus inducing the progressive loss of photoreceptors (Thomas et al., 2016).

Retinal Organoid Development and Transplantation

CSC-14 human embryonic stem cells (Aivita Biomedical Inc.) were grown and expanded using Stem Blast media (Irvine Scientific) and supplement. These are both chemically defined and xeno-free. The media contained low levels of FGF and Activin-A and the cells were grown on thin Matrigel and passaged every 3–4 days at 1:6 to 1:10 splits using Collagenase IV digestion. For differentiation, cells were digested with Collagenase IV and the media was replaced with Stem Blast+B27 (Gibco). Aggregates were allowed to form embryoid bodies in low adherence dishes. Media was replaced every two days and after 7–10 days, the cells were cultured on a laminin-collagen substrate. After 21–28 days, "horseshoe" shapes appeared and these structures were separated and dissected. These structures, called retinal organoids, were then placed in a suspension culture until time of transplantation (method after Zhong et al., 2014).

Retinal organoids that were transparent, contained an RPE "blob," and had a regular shape with laminar organization were cut into rectangular shaped pieces (0.8–1.2 x 0.6 mm).

The transplantation technique used to place the retinal sheets is described elsewhere (Seiler et al., 2017).

Perfusion and Immunohistochemistry

Rats were perfusion-fixed using chilled 4% paraformaldehyde in a 0.1 M Na-phosphate buffer. Once complete, their eyes were harvested, the eye cup was cut along the dorsoventral axis, and the cornea was removed. The dissected eye cups were kept in a 30% sucrose solution overnight, then were embedded into an O.C.T.™ compound, frozen using isopentane on dry ice and stored at -80°C. The blocks were then cut into 10-micrometer sections and placed on slides (three sections per slide), which were stored at -20°C. Every fifth slide was stored at 4°C for H and E staining. The slides were then stained with hematoxylin and eosin before they were dehydrated. They were then mounted using a 1:2 (Clear-rite: Paramount) solution and stored at room temperature, before being analyzed under a light microscope at 10X and 40X.

For immunohistochemistry using diaminobenzidine (DAB) as a substrate, the slides were dried for an hour at 37°C, and then placed in 1X Histo VT (1:10 dilution, Nacalai, Inc., San Diego, CA, USA) at 70°C for 30 minutes for antigen retrieval. The slides were washed with 1X PBS (phosphate-buffered saline: 0.1 M NaCl, 0.05 M Na-phosphate buffer, pH 7.2), and the sections blocked with a mixture of 20% horse serum (majority is PBS/1%BSA/0.3 Triton) for 30 minutes. Slides were then incubated in primary antibodies overnight at 4°C. The primary antibodies used were mouse anti-Rhodopsin (1:10,000; clone Rho1D4, Dr. Molday, Univ. of British Columbia), mouse anti-SC121 (1:25,000; Stem Cell Inc., Newark, CA), rabbit anti-Recoverin (1:15,000; Millipore), rabbit anti-Ku80 (1:500; Abcam, Cambridge, MA), and rabbit anti-Red/Green Opsin (1:2000; EMD Millipore, Billerica, MA). These stained rod cells, human cytoplasmic proteins, photoreceptors and cone bipolar cells, human nuclei, and red and green cone cells, respectively. After extensive washing with PBS, secondary antibodies (biotin-horse-anti-mouse-IgG [1:400] and biotin-horse-anti-rabbit [1:400], depending on the primary) were applied for 30 minutes. After washing, Elite ABC was applied and incubated for 45 minutes, and then the Vector DAB kit was applied for 2–3 minutes. The slides were then mounted using gelatin mounting media and imaged using an Olympus BXH10 (Cypress, CA, USA).

For immunofluorescence (IFA) imaging, slide preparation and blocking were done in a similar way to the DAB staining, except that donkey serum was used. The primaries used were mouse anti-SC121 (1:500; Stem Cell Inc.; specific for human cytoplasm), in combination with rabbit anti-Red/Green Opsin (1:500; Oxford Biomedical, Oxford, UK), rabbit anti-Recoverin (1:1000; EMD Millipore), or mouse anti-Rhodopsin (1:1000; Molday). In addition, we used goat anti-Synaptophysin (1:100; Novus Bio, Littleton, Colorado) in combination with mouse anti-PKC (1:50; Stressgen, Ann Arbor Michigan) and rabbit anti-Ku80 (1:400) or rabbit anti-Synuclein (1:100; Cell Signaling, Danvers, MA) and mouse anti-SC121 (1:1000). After washing, the light-sensitive secondary antibodies were applied in the dark and incubated for 30 minutes. RhodX-donkey anti-mouse-IgG (red; 1:400), AF488-donkey-anti-rabbit-IgG (green; 1:400), and AF647-donkey-anti-goat-IgG (magenta; 1:400) were the secondary antibodies used. The sections were then mounted with DAPI anti-fade fluorescent mounting medium (Vector) and sealed with nail polish. Slides were imaged on an LSM700 confocal microscope (Carl Zeiss Microscopy GmbH, Oberkochen, Germany). Confocal stacks were 5–8 micrometers and images were done at 40X. Zen 2012 software was used to extract the images. Images for DAB staining and IFA were analyzed once the image processing was complete.

Results

DAB Staining Results

Figure 1 demonstrates the presence of photoreceptors and cone bipolar cells in an RCS rat that was perfused 217 days post-surgery (DPS). The images were taken from adjacent sections. There are noticeable rosettes containing photoreceptors within the transplants (indicated by the black arrows). Rosettes are defined as photoreceptor layers around a lumen, surrounded by other retinal layers. The

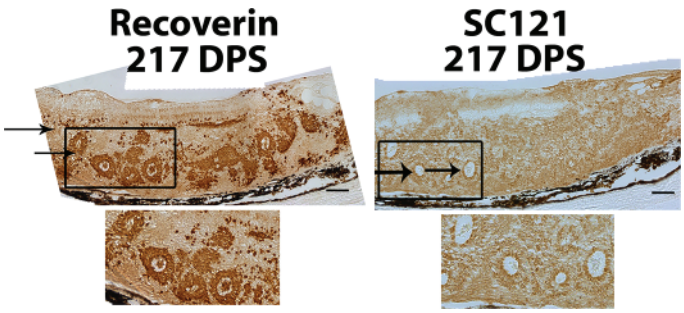

Figure 1

DAB Staining with Recoverin and SC121. This figure depicts the result of DAB staining with Recoverin, which stains photoreceptors and cone bipolar cells, and SC121, which stains proteins in human cell cytoplasm. Therefore, Recoverin visualizes photoreceptors in the transplant, while SC121 visualizes the location of the transplant (human cells). The black arrows indicate rosettes. Both images are from the same slide of a rat that was perfused 217 days post-surgery (DPS). The scale bar represents 100 microns.

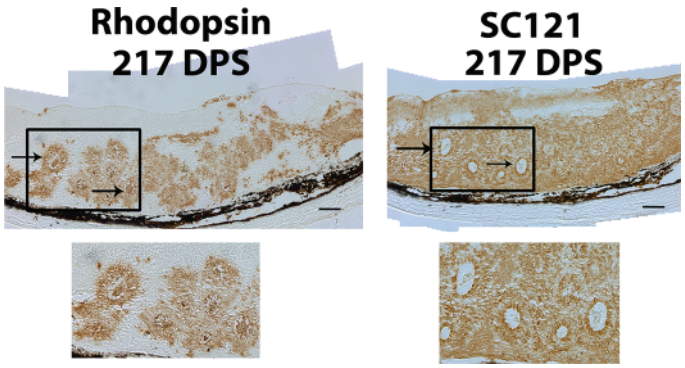

Figure 2

DAB Staining with Rhodopsin and SC121. This figure depicts the result of DAB staining with Rhodopsin, which stains rod cells, and SC121, which stains proteins in human cell cytoplasm (same rat subject as Figure 1). Rhodopsin is used to visualize rods in the transplant, while SC121 visualizes where the transplant (human cells) is. The black arrows indicate rosettes. The scale bar represents 100 microns.

Recoverin antibody primarily stained portions of the transplant (visualized with SC121), so photoreceptors seen were associated with the transplant.

Figure 2 depicts the presence of rod cells within the same transplant on adjacent sections (same part of the transplant). By comparing the sections, it was clear that rod cells (where Rhodopsin stained) were contained to the transplanted region. Rosettes can also be seen in both images.

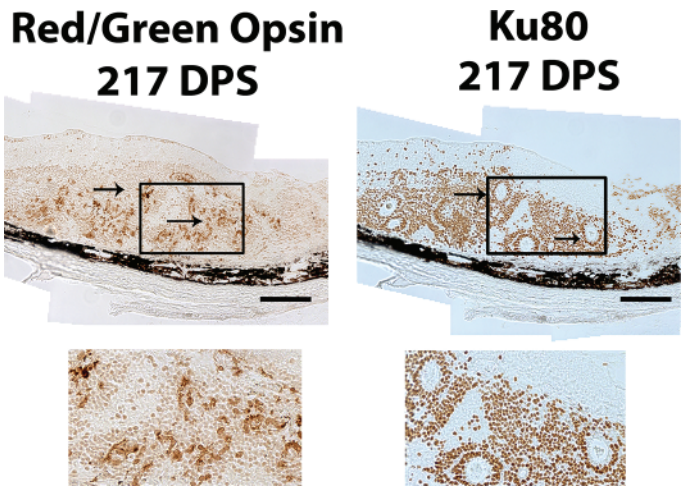

Figure 3

DAB Staining with Red/Green Opsin and Ku80. This figure depicts the result of DAB staining with Red/Green Opsin, which stains red/green cone cells, and Ku80, which stains proteins in human cell nuclei (same rat subject as Figure 1). Red/Green Opsin visualizes where red and green cones formed in the transplant, while Ku80 visualizes the location of the transplant (human cells). The black arrows indicate rosettes. The scale bar represents 100 microns.

The red/Green Opsin antibody (Figure 3) visualizes red and green cone cells and shows again that they are concentrated in the transplanted region. Ku80 visualizes human nuclei of transplant cells, so its purpose is similar to SC121. Rosettes can also be seen. Looking at Recoverin, Rhodopsin, and Red/Green Opsin, a thick layer of photoreceptors can be seen. This layer was clearly formed from the RPC transplanted layer, since they do not seem to be derived from host tissue.

Figures 4 and 5 compare a human embryonic stem cell (hESC)-derived RPC sheet and the human fetal sheet transplant, stained with Recoverin (Figure 4) and Rhodopsin (Figure 5). The sections are from two different rats with similar day post-surgery (DPS) values. Rosettes can be seen in all sections, as well as a similarity between structure and abundance of photoreceptors between the hESC-derived transplant and the human fetal retinal transplant.

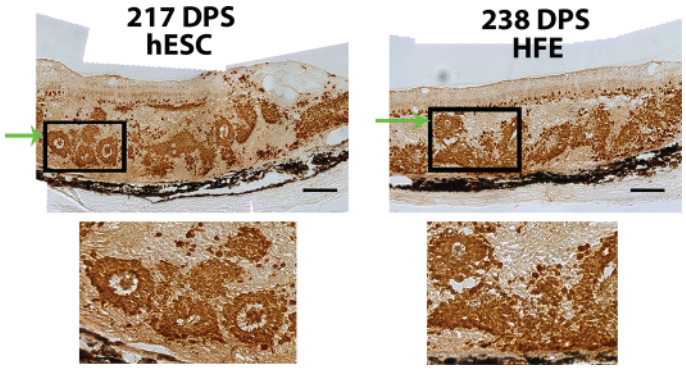

Figure 4

DAB Staining with Recoverin on Two Different Types of Transplants. Right: Human fetal retina (HFE); left: hESC-derived retina, in two different rats. Both are stained with Recoverin, which visualizes photoreceptors and cone bipolar cells. The green arrows indicate rosette formation. The scale bar represents 200 microns.

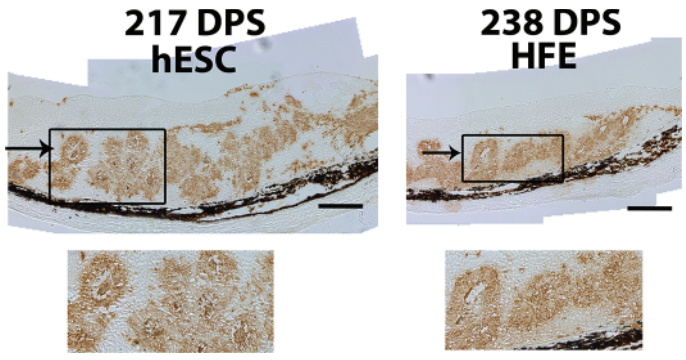

Figure 5

DAB Staining with Rhodopsin on Two Different Transplants. Left: hESC-derived retina; right: Human Fetal Retina (HFE). Both are stained with Rhodopsin, which visualizes rod cells. The black arrows indicate rosette formation. The scale bar represents 200 microns.

Immunofluorescence (IFA) Results

Figures 6 and 7 focus on how the transplant grew and differentiated over time. Figure 6 visualizes Rhodopsin, which stains rod cells. In Figure 7, both sections were stained to visualize Recoverin, which marks cone bipolar cells and photoreceptors. However, in both figures, the image on the left is from a rat that was perfused much earlier than the image on the right. The right image demonstrates a more advanced development of the photoreceptor layer. However, rosettes are present in both transplants. A thin layer of host photoreceptors can be seen in the left image, but is completely absent in the right image in both figures.

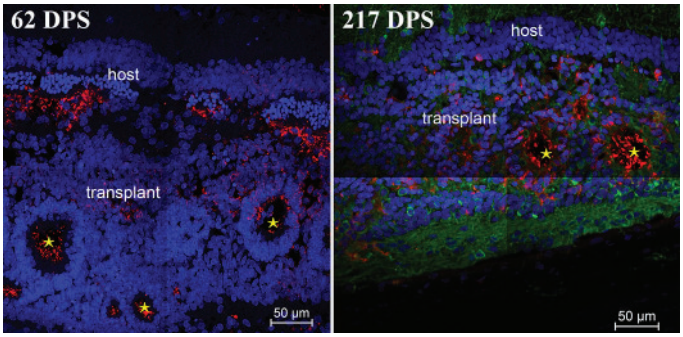

Figure 6

IFA Staining with Rhodopsin, SC121, and DAPI, comparing two transplants of different ages (62 and 217 dps). Rod cells Rhodopsin (red), nuclei: DAPI (blue), human cytoplasm: SC121 (green, 217 dps only). Rosettes can be seen in both images (yellow asterisks indicate rosette lumen). Host rod cells (red) can be seen in the left image. The scale bar represents 50 microns.

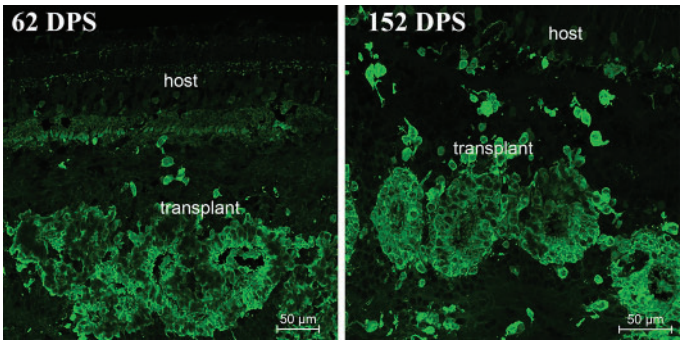

Figure 7

IFA Images after Recoverin Staining of Transplants. This figure demonstrates how the transplant differentiates and grows over time. Both images are taken from RCS rats with implanted hESC-derived RPC sheets. The left image is from a rat that was 62 DPS and the right is from a 152 DPS rat. Both sections were stained and imaged to visualize photoreceptors and cone bipolar cells (Recoverin). In the left image, one can see a thin layer of host photoreceptors (visualized by the green towards the top of the image) while in contrast these are absent later during development and the only photoreceptors are found in the transplant. The scale bar represents 50 microns.

Figures 8 and 9 demonstrate the integration of the host layer and the transplant layer. Figure 8 visualizes Ku80, which identifies human nuclei, and PKC, which identifies rod bipolar cells. Synaptic vesicles are visualized in gold by the Synaptophysin antibody. In Figure 9, α-Synuclein, which stains rat inner plexiform layer (IPL) and amacrine cells, and SC121, which stains human cytoplasm are visualized. Synaptophysin is also visualized as gold. In both Figures, there is a much more significant amount of gold staining in the host IPL layer in the 152 DPS section, compared to the 62 DPS.

Figure 10 contain images processed using Volocity software (www.cellularimaging.com) and is a 3D visualization of the synapses from Figure 8. There is an increased amount of

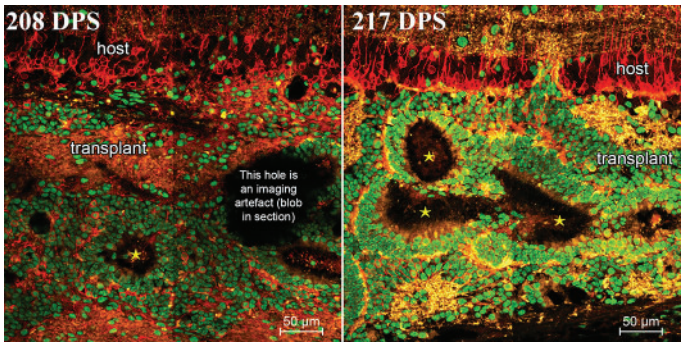

Figure 8

IFA Imaging of PKCα (rat rod bipolar cells), Ku-80 (human nuclei) and Synaptophysin (synapses) Staining. Confocal imaging was used to visualize rod bipolar cells (red), human nuclei (green) and synaptophysin (yellow). Both transplants contained photoreceptor rosettes (yellow asterisks). Synaptophysin processes extend into the inner plexiform layer of the host. The scale bar represents 50 microns.

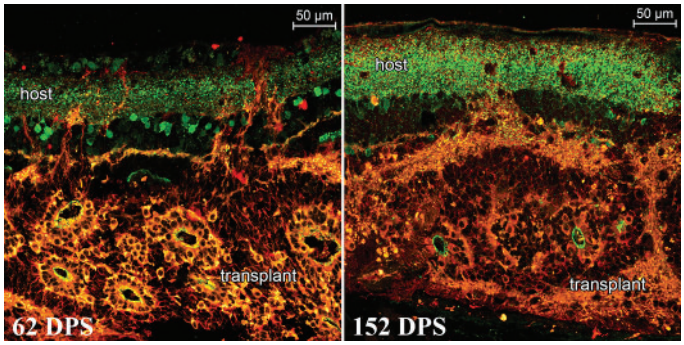

Figure 9

IFA Staining with rat-specific α-Synuclein, SC121, and Synaptophysin. Human cytoplasm: SC121 (red); rat host IPL and amacrine cells: α-Synuclein (green); synaptic vesicles: Synaptophysin (gold). Note the increase of synaptophysin and extension of SC121 and transplant processes in the inner plexiform layer of the host retina. Scale bar represents 50 microns.

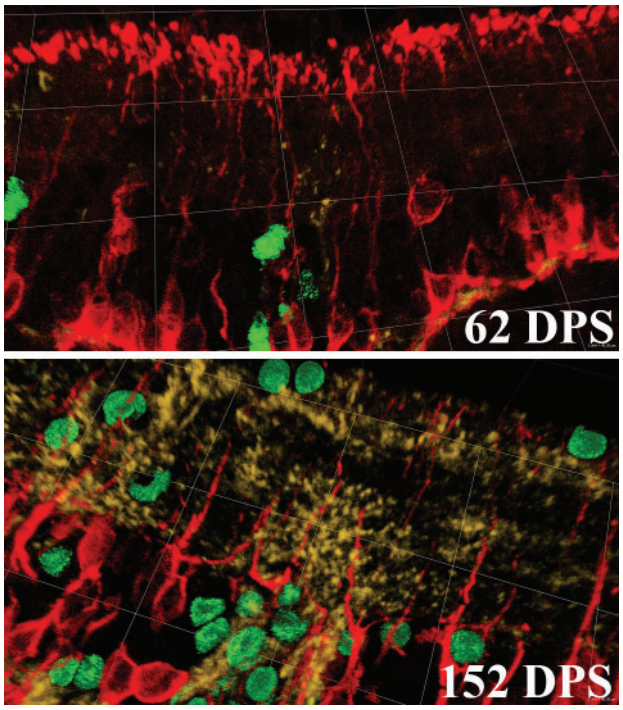

Figure 10

3D Visualization of PKC, Ku80, and Synaptophysin. Top image: 62 DPS rat, bottom image: 152 DPS rat. The bottom image portrays more synaptic connectivity between the host rod bipolar cells (PKC alpha, red) and the transplant (human nuclei, green; and synaptophysin, gold). The grid contains 10 by 10 micrometer squares for scale.

gold staining in the PKC host (rat) layer in the 152 DPS image, when compared to the 62 DPS image.

Discussion

Figures 1, 2 and 3 all demonstrate that the transplanted sheet differentiated into rosettes of retinal cell types. Previous studies with RCS rats have shown a complete degeneration of the RPE and photoreceptor layers in the later stages of retinal degeneration, meaning that without the transplant, photoreceptors, like rods and cones, should not be present in significant amounts (Mullen and LaVail 1976; Adachi et al., 2016). This degeneration of the photoreceptor layer is what makes RCS rats so valuable to research, since a lack of a responsive photoreceptor layer is also the result of retinal degeneration in humans (Cuenca et al., 2005). The DAB staining used to visualize human cells (SC121 and Ku80) indicates where the transplant is and it can be clearly seen that most of the photoreceptors (visualized with Recoverin, Rhodopsin, and Red/Green Opsin) are concentrated within that layer. Therefore, the presence of photoreceptors in RCS rats must be primarily due to the transplant. Figures 6 and 7 also lead to a similar conclusion, since they do show the development of rod (seen by Rhodopsin staining) and cone (seen by Recoverin) cells in the transplanted region. One can also see that the transplant region is significantly more developed, in terms of number of photoreceptors, in the 152 DPS image than the 62 DPS image.

Looking at Figures 6 and 7 it is clear that the number of photoreceptors and rod bipolar cells increased over time. This is notable because, as previously mentioned, the number of photoreceptors in RCS rats should decrease over time. The degeneration of the host photoreceptors is also very apparent in both figures. The image on the left has a small amount of Recoverin staining (towards the top of the image), which demonstrates that host photoreceptors remain in younger RCS rats. If one looks at the image on the left, there is no such portion of Recoverin staining that is strictly associated with the host. All of the Recoverin staining is concentrated in the transplant region, since the host photoreceptors have completely degenerated. The same can be seen in Figure 6 with Rhodopsin staining. This supports the hypothesis that the transplant significantly increased the number of photoreceptors present in rat hosts that would have otherwise been void of photoreceptors.

The integration between the transplant layer and the host layer can be seen in Figures 8 and 9. In both images, one can see that, in younger rats, Synaptophysin (synaptic vesicles) and SC121 (human cell processes) staining is contained to the transplant layer. This is intuitive, as one would expect to see human processes propagating between human cells. In the older rats, however, the notable portion is that the Synaptophysin staining has increased in intensity in the host layers. This is interesting because we see human SC121 processes between rat cells, meaning that the two layers must be communicating, Figure 9 demonstrates a clearer view of this communication because it suggests the presence of increased Synaptophysin staining between the host rod bipolar cells and the transplant nuclei.

In addition, the formation of rosettes, which occurred in all retinal organoid transplants, is another notable occurrence. Previous studies have found that rosette formation is associated with lower visual acuity than if the transplant differentiated into horizontal layers of retinal cells. However, transplants containing only rosettes were still found to increase visual acuity when compared to controls (Seiler et al., 2017). The formation of rosettes could be due to trauma to the tissue during cultivation or transplantation (Seiler et al., 2009). Rosette formation could also have been due to the type of transplant. Looking at Figures 4 and 5, there seems to be a slight difference between the embryon-

ically derived transplant and the human fetal retinal (HFE) transplant. The HFE transplants seem to be, overall, more laminar and less rosetted, meaning that they may be associated with better responses (Seiler et al., 2017). In any case, additional research must be done in order to establish if hESC-derived transplants result in more rosette formation in RCS rats than HFE transplants. In spite of the development of rosettes, the transplants still developed retinal layers (Seiler et al., 2017).

Conclusion

Future studies must be done in order to establish that all the layers of the retina have been properly formed and integrated. This study focused on the development of photoreceptors, rather than a full retina and its many layers. Additional staining must be done to demonstrate presence of additional retinal cells, such as ganglion cells, RPE, rod bipolar cells, microglia, Muller cells, etc. These future experiments would provide valuable information on how complete the differentiated transplant is.

Future studies should also include Optokinetic (OKN) Response Testing in order to correlate the presence of photoreceptors to visual acuity. Although the presence of photoreceptors is associated with an increase in visual acuity, having OKN data will provide a direct link. Finally, future studies should include a larger subject pool, with varying age groups. This will not only provide us with more cohesive data and eliminate outliers, it will also provide more information on how the transplant grew over time. In addition, a larger subject pool will also help establish if rosette formation was due to the hESC-derived transplant or just trauma during surgery. With clinical research in mind, further improvement of this research can be used in finding the solution for retinal diseases such as age-related macular degeneration, since our study has proven that the transplantation of retinal organoid sheets leads to the development of photoreceptors.

Acknowledgements

We would like to thank Dr. Magdalene Seiler for preforming the actual transplant surgery, as well as her support and guidance throughout the process. We would also like to thank Bryce McLelland and Anuradha Mathur who not only acted as mentors, but also assisted with perfusing the rats, the experimental design, and the analysis of the results. We would like to also thank Kian Iraninejadian, Tina Karimi, Andrew Asoo, and Elyse Corpuz for assisting with cutting and staining the sections.

Works Cited

Adachi K, et al., 2016. Optical Coherence Tomography of Retinal Degeneration in Royal College of Surgeons Rats and Its Correlation with Morphology and Electroretinography. *PLoS ONE* 11(9): 1–16.

Cuenca N, et al., 2005. Early changes in synaptic connectivity following progressive photoreceptor degeneration in RCS rats. Eur. *J. Neurosci.* 22:1057–1072.

D'Cruz P, et al., 2000. Mutation of the receptor tyrosine kinase gene Mertk in the retinal dystrophic RCS rat. *Human Molecular Genetics* 9(4): 645–651.

Lie MM, et al., 2011. Gene therapy for ocular diseases. *Br. J. Ophthalmol.* 95:604–612.

Lim LS, et al., 2012. Age-related macular degeneration. *Lancet* 379:1728–1738.

McLelland et al., in revision. Transplanted hESC-retina organoid sheets differentiate, integrate and improve visual function in retinal degenerate rats. *Invest. Ophthalmol. Vis. Sci.*, submitted.

Molday RS, MacKenzie D. 1983. Monoclonal antibodies to rhodopsin: characterization, cross-reactivity, and application as structural probes. *Biochemistry* 22:653–660.

Mullen R, LaVail M. 1976. Inherited Retinal Dystrophy: Primary Defect in Pigment Epithelium Determined with Experimental Rat Chimeras. *Science* 192:799–801.

Radtke, et al., 2008. Visual Improvement in Retinal Degeneration Patients by Implantation of Retina Together with Retinal Pigment Epithelium. *Am. J. Ophthalmol.* 146(2):172–182.

Seiler M, et al., 2009. Functional and structural assessment of retinal sheet al.lograft transplantation in feline hereditary retinal degeneration. *Vet. Ophthalmol.* 12:158–169.

Seiler MJ, Aramant RB. 2012. Cell replacement and visual restoration by retinal sheet transplants. *Prog. Retin. Eye Res.* 31:661–687.

Seiler et al., 2014. A new immunodeficient pigmented retinal degenerate rat strain to study transplantation of human cells without immunosuppression. *Graefe's Arch. Clin. Exp. Ophthalmol*, 252:1079–1092 (2014). DOI 10.1007/s00417-014-2638-y.

Seiler MJ, et al., 2017. Vision Recovery and Connectivity by Fetal Retinal Sheet Transplantation in an Immunodeficient Retinal Degenerate Rat Model. *Invest. Ophthalmol. Vis. Sci.* 58:614–630.

Thomas B.B. et al., 2016. A new immunodeficient dystrophic RCS rat model for transplantation studies using human derived cells. Invest. Ophthalmol. Vis. Sci. 56: *ARVO E-abstract* 3735

Zhong X, et al., 2013. Generation of three-dimensional retinal tissue with functional photoreceptors from human iPSCs. *Nature Communications* 5:4047. doi: 10.1038/ncomms5047.